EXPERIMENTAL TECHNIQUES FOR THE MEASUREMENT OF RELATIVE PERMEABILITY AND IN-SITU SATURATION IN GAS CONDENSATE NEAR WELL BORE AND DRAINAGE STUDIES

Andrew Cable, Robert Mott and Mike Spearing (AEA Technology plc)

ABSTRACT

Well deliverability in most gas condensate reservoirs is reduced by condensate banking when the pressure falls below the fluid dew point, but the impact of condensate banking may be reduced due to improved mobility at high capillary number in the near-well region. Fevang and Whitson [1] have shown that the key parameter in determining well deliverability is the relationship between k_{rg} and the ratio k_{rg}/k_{ro}. They also suggested an experimental technique for measuring k_{rg} as a function of k_{rg}/k_{ro} using core plugs.

We have applied the experimental pseudo steady-state technique to reservoir core at high pressure and temperature, measuring relative permeabilities under conditions which are similar to the near-well region of a gas condensate reservoir. With this technique it is possible to measure all of the relative permeability data needed to predict well deliverability, including the increase in mobility at high capillary number. We describe the experimental techniques, and present results for a sandstone core from a North Sea gas condensate reservoir, using a 5-component synthetic fluid. The results show a clear increase in mobility with capillary number, at flow rates which are typical of the near-well region. The dependence of k_{rg} on k_{rg}/k_{ro} can be used directly in pseudopressure methods to calculate well deliverability. We also describe how the data for k_{rg} versus k_{rg}/k_{ro} can be used to define parameters for empirical correlations of relative permeability versus saturation, so that the results can be used in reservoir simulators.

The pseudo steady-state technique measures relative permeabilities and does not require saturations to be measured. However for the correct interpretation of coreflood data for relative permeability analysis, in-situ saturation information is recommended. In recent years, with the increasing importance of condensate reservoirs, x-ray methods have been developed with a view to making quantitative in-situ saturation measurements on condensate systems, although this is difficult due to the inherent small density difference between the gas and liquid phases. We describe the x-ray apparatus and the techniques necessary to achieve the high repeatable accuracy required for condensate in-situ saturation measurements. Two-phase condensate/gas in-situ measurements are presented for a high pressure condensate drainage experiment in a vertical long core. This was a commissioning study for the x-ray scanner and used an iodo-decane dopant to increase saturation accuracy. Studies are being extended to in-situ saturation measurements during the pseudo steady-state stage of the near well bore condensate measurements. The saturation accuracies of the condensate liquid and gas have been predicted to be ± 2% PV at the bottom hole flowing temperature and pressure, without the use of high density dopants in either phase.

1. INTRODUCTION

Gas condensate reservoirs are usually developed by pressure depletion which leads to condensation within the reservoir. Well deliverability may be reduced by condensate banking when the pressure falls below the fluid dew point. However, the impact of condensate banking on well deliverability can be reduced by improved mobility at high capillary number in the near well region.

There are a number of physical processes that are important in determining well productivity. The balance of processes that reduce productivity (e.g. condensate banking, non-Darcy flow) and those that may increase productivity (e.g. high capillary number flow, water vaporisation) is not well understood. In the near well bore region, viscous forces will dominate, and the large pressure drop will cause an accumulation of condensate liquid resulting in high local saturations. The local condensate saturation may significantly

reduce the gas permeability and will dictate the number of wells required to fulfil a gas sales contract. However, experience in several gas condensate reservoirs suggest that well productivity losses are less severe than predicted by simulation models [2,3]. This may be attributed to inappropriate relative permeability data from conventional steady-state low pressure measurements, which do not take account of reservoir condition retrograde condensation and relative permeability rate dependencies.

This paper describes the techniques used to measure high rate condensate relative permeabilities using gas condensate fluids with the liquid phase introduced by condensation. The competing effects of high capillary number and non-Darcy flow are investigated. The paper also describes an in-situ saturation measurement technique by x-ray attenuation and presents saturation data from a commissioning, condensate drainage experiment. The experience gained from this and other studies is being applied to high rate, near well bore experiments to measure the steady-state condensate saturation.

2. EXPERIMENTAL EQUIPMENT

2.1 Condensate Module

The study was carried out using the 'Condensate Module' which is a reservoir condition facility with design conditions of 150°C and pressures up to 690 barg (10,000 psig). The module is housed in an oven and custom-built to allow the use of x-ray in-situ saturation monitoring. The set up is shown in Figures 1 and 2. For low flow rate gas condensate measurements, one litre pistonless accumulators are used to contain the test fluids; two inlet vessels and one outlet vessel all contained inside the oven at test conditions. Water was used as the driving medium by means of positive displacement pumps (two injection pumps and one extraction pump). Using water as the motive fluid allows the process fluids to equilibrate and minimises the occurrence of brine stripping from the core during high throughput gas flooding. Low x-ray attenuating carbon composite or aluminium core holders were used to contain the core material in a vertical orientation. A long windowed PVT cell was included in the flow circuit between the core and the outlet vessel for measurement of core effluent and gas condensate PVT characteristics. Pressures and temperatures were monitored and recorded by means of a data logging system.

2.2 Near Well Bore Flow Circuit

The near well bore flow circuit was designed to undertake measurements using a pseudo steady-state method first outlined by Fevang & Whitson [1]. The aim was to measure gas relative permeability (k_{rg}) as a function of k_{rg}/k_{ro} at high flow rates typical of the near well bore region. The flow circuit has a maximum operating temperature of 80°C and core confining pressure of 275 barg (4,000 psig). These constraints, and hence the use of a synthetic gas condensate, were imposed by use of an aluminium core holder, chosen for its low x-ray attenuation. Gas condensate flowrates in excess of 10 L/h have been achieved with this set up. A schematic diagram of the flow circuit is given in Figure 2.

The flow circuit uses an inlet piston accumulator of 15 L capacity to contain the test fluid at a given pressure (P_1) and composition. The pressure of this vessel is kept constant by injection of water. An outlet 15L piston accumulator is used to contain effluent fluid from the core, which first passes through a long-windowed PVT cell. The cell enables the flowing condensate phase to be measured. High rate operation is achieved by setting an outlet vessel pressure (P_3) using a PC-controlled back pressure regulator and maintaining a constant core inlet pressure (P_2) using a PC-controlled pressure reducing regulator. The single phase fluid contained in the inlet accumulator flashes across the inlet pressure reducing regulator, by as much as 70 barg (1000 psig) to introduce two-phase flow into the core. Water eluted from the outlet 15 L piston accumulator is measured to obtain the total flowrate. The established flowing condition is maintained at a constant core differential pressure until a steady-state flowing condensate/gas ratio is obtained and measured. The flow circuit is operated as a sealed system and the fluid is recycled for the duration of the study.

2.3 X-ray Scanning Platform

The facility is shown schematically in Figure 3 and comprises a rigid gantry assembly which supports the vertical translational system of x-ray tube and detector. The experimental module is mounted on a 3.8 m long platform which can be positioned to within 100 μm relative to the x-ray/detector system. The x-ray scanner enables high resolution saturation information to be generated and has the capability to operate in both single and dual energy modes. This allows 2-phase and 3-phase data to be collected. Sequences can be programmed so that scanning can be automatically performed overnight. The computer-controlled x-ray system provides a high photon flux, high stability and low ripple x-ray generation. The line array detector system allows a 0.5 mm resolution over a 512 mm field of view using 1024 detector elements. The detector shows excellent repeatability (to approximately 0.02%) which is essential for 3-phase or condensate studies. The detector head can be rotated by 90° allowing horizontal or vertical measurements.

For the condensate drainage study, the scanner was set-up to take data horizontally at 30 positions along the vertical core with a slice height of 5 mm and an interval of 3 cm between each scanning position, thus covering the complete core length. For the high rate tests the detector was set up in a vertical orientation to increase the speed of a scan. In this way the complete length of the core can be scanned in one exposure. To cover the majority of the pore space (~87%), four vertical lines were taken, each of 6.4 mm width.

2.3.1 X-Ray Normalisation

The x-ray beam is subject to long term drift, short term ripple and fluctuations on the individual detector elements. To combat this the raw x-ray data has to be normalised. Two forms of normalisation are used. A measurement on a piece of aluminium, sized to be of equal attenuation as the core/coreholder system, is taken at the same time as each core measurement (for each line of data), the aluminium covering a small number of detector elements at one end of the detector array. This is referenced to a measurement made at the start of the test to give an 'edge' normalisation factor. At the start of a core scan sequence, a measurement is made on a piece of aluminium covering the full 512 mm field of view. This is referenced back to a measurement made at the start of the test to give 'white' normalisation factors for each detector element. In this way all detector changes are allowed for and experiments lasting many months are directly comparable.

2.3.2 X-Ray Data Accuracy

The statistical accuracy demanded from the x-ray scanner depends upon (a) whether the study is a 2-phase or 3-phase test and (b) the in-situ fluid saturation accuracy required. 3-phase tests require a much higher level of statistical accuracy for a given fluid saturation accuracy because six calibrations at two energies are required compared with two calibrations at one energy for a 2-phase test [4].

In practice, the saturation accuracy is constrained by three factors: (a) the difference in linear attenuation coefficient of the fluids, which depends to a large extent on the densities of the fluids (with condensate systems, the density difference between liquid and gas phases is inherently small, which leads to either long scan times or poor saturation accuracies), (b) time limitations, whether it is a scan during dynamic flood or at steady-state, and (c) the desired spatial resolution of the data.

The above factors have to be taken into account when defining a scanning program for a core flood study. The factors are optimised to obtain good in-situ saturation accuracy in a practical time frame. At reservoir conditions, oven walls and high pressure core holders dictate higher x-ray energies just to penetrate the target. Longer x-ray scan times are also required to achieve a given count rate, and at higher energies the fluids attenuate less causing an even smaller linear attenuation difference between the fluids. All these issues contribute to the complexities of producing accurate saturation measurements on condensate systems.

Where low attenuation differences between fluids exist in oil-water systems, high x-ray attenuating dopants can be added to increase the fluid saturation accuracy. However, the addition of dopants is undesirable in condensate systems as the effect on the PVT characteristics of the fluid is unknown; and equation of state PVT simulations tend not to include dopant elements such as iodine or tungsten. For the near well bore test dopant was not used to avoid the need for a PVT study on the 5-component fluid. To estimate the saturation accuracy for the near well bore test, we have developed spreadsheet tools that allow the factors mentioned above to be modelled for both 2-phase and 3-phase tests [4]. Using these tools, the predicted saturation error for 3-phase tests on a condensate system was up to 16% PV given the experimental constraints, see Figure 4. The analysis for the 2-phase case (assuming immobile water) showed that saturation accuracies of ~ 2% PV could be achieved in one or two hours, see Figure 5. Both 2-phase scans use a 15 second shutter time, but the former repeats the measurement 30 times on each of the 4 lines of data, while the latter repeats the measurement 60 times.

The polychromatic nature of x-rays leads to 'beam hardening' when penetrating material, an additional factor which affects the measured saturation. A suite of software codes has been developed to model the beam hardening process, and we have found in a variety of 3-phases tests that, with 1.5" diameter cores, beam hardening causes a discrepancy of only about 2% saturation with typical doped fluids (3% NaI in brine or 20% iodo-decane). The effect depends on many factors, in particular the concentration of dopant, type of dopant and fluid thickness (core diameter). In 2-phase undoped tests, such as the condensate system in the present study, the effect of beam hardening on the saturation has been found to be negligible. A 0.56 mm copper filter has been used in the present test to pre-harden the beam and further reduce the effect of beam hardening.

For the condensate drainage test, iodo-decane dopant ($C_{10}H_{21}I$) was used to increase saturation accuracy, as it was a commissioning test and the fluid PVT characteristics were not important. The predicted saturation accuracy was 2.7% PV which compares well with the experimental data presented in Section 5.

3. GAS CONDENSATE FLUIDS

For the near well bore experiment, a 5-component synthetic gas condensate was used. The composition of the fluid is given in Table 1. The properties of this fluid have been predicted using a tuned EOS model at temperatures of 40°C, 60°C and 80°C to provide fluid characteristics, viscosity and interfacial tension (IFT). The fluid properties have also been measured. Predicted constant composition expansion (CCE) and measured constant volume depletion (CVD) data is given in Figure 6. For this fluid, the IFT and maximum condensate saturation can be conveniently controlled by choice of temperature.

COMPONENT	**5-C FLUID** Mol %	**5-C FLUID** Weight %	**6-C FLUID** Mol %	**6-C FLUID** Weight %
Methane	80.0	45.59	80	52.3
Ethane			11	13.5
n-Butane	14.0	28.88	4	9.5
Heptanes	4.0	14.24	3	12.3
Decanes	1.4	7.07	1.4	8.1
Dodecanes			0.6	4.2
Tetradecanes	0.6	4.22		

TABLE 1 - MODEL CONDENSATE COMPOSITION

For the gas condensate drainage experiment, a 6-component synthetic condensate was used. This fluid was designed to be a rich gas condensate at laboratory temperature. To increase the accuracy of x-ray in-situ saturation measurements, the fluid was doped by replacing 25% wt of the decane component with

iodo-decane. EOS simulation for the undoped fluid predicted a dew point of 215 barg at 20°C with a maximum liquid dropout of 24% at 186 barg. The measured properties of the doped fluid were appreciably different (although the fluid did remain a gas condensate); the dew point was shifted to 225 barg at 20°C with a maximum liquid dropout of 21% at 130 barg.

4. CORE MATERIAL

Clashach outcrop sandstone was used in the drainage experiment, and its properties are shown in Table 2. A relatively high permeability sample was used so that gravity drainage would be promoted if it was to occur. The core was flooded to S_{wi} by humidified gas flooding at ambient conditions. For the near well bore experiment, a North Sea sandstone was used. The core was CT scanned to ensure a homogeneous sample was selected and flooded to S_{wi} using a porous plate technique. Core properties are given in Table 2. Prior to the near well tests, the core was extensively used for the measurement of gas condensate relative permeability at conditions appropriate to the deep reservoir. The core had therefore been restored by core aging in real fluid at reservoir conditions prior to use.

Description	**Outcrop Core**	**Reservoir Core**
Mean Length (cm)	88.0	25.8
Mean Diameter (cm)	4.10	3.80
Mean Area (cm^2)	13.2	11.3
Bulk Volume (cm^3)	1161.8	291.5
Pore Volume (cm^3)	232.6	74.0
Porosity (%)	20.0	25.4
Abs Brine Permeability (md)	762	102.4
S_{wi} (PV)	0.321	0.118
K_e – Reference (md)		67.7

TABLE 2: CORE CHARACTERISATION DATA.

5. RESULTS FROM CONDENSATE DRAINAGE EXPERIMENT

The flow circuit was set up so that the outlet vessel, PVT cell and the core were on line to the inlet condensate vessel, Figure 2. A depressurisation was performed on the system over a two day period from 270 barg to 160 barg. Following depressurisation and fluid equilibration, the PVT cell was observed for 16 days and no change in condensate volume was recorded , the liquid volume remaining at 15.5% of the sample volume at dew point. Throughout the duration of the test, 2-phase in-situ saturation scans were performed to monitor the drainage of condensate. No condensate drained from the core into the PVT cell .

Saturation data from nine scans taken throughout the drainage test are plotted in Figure 7 and qualitative images are shown in Figure 8 illustrating liquid drainage and condensate banking at the outlet of the core. The scans in Figure 7 only show the saturation of a 5 mm strip down the centre of the core. Drainage was still evident after 16 days. The measured condensate saturation in the 5 mm view decreased from 30.5% to 26% during the drainage, although no oil was produced into the PVT cell. This may be taken as evidence that the local view in the centre of the core is not indicative of the average core saturation. The final average oil saturation of the core was 26% HCPV from the in-situ measurement, which exceeded the 15.5% CVD as measured in the PVT cell. This has been attributed to a methane gas calibration when in fact an equilibrium condensate gas ideally should have been used. It has been shown analytically that a uniform 1% decrease in the gas calibration grey levels caused the scanner saturations to equal mass balance results. The calibration error would lead to a systematic error in all saturations. Therefore saturations shown in Figure 7 could be shifted down by approximately 10% to match the mass balance, and the estimated trapped gas saturation at the outlet would be in the region of 40% to 50%.

6. RESULTS FROM NEAR WELL BORE EXPERIMENT

6.1 Test 1: Single Phase Measurements ~230 bara

The first high rate experiment investigated non-Darcy flow with the 5-component fluid above the measured dew point pressure of ~212 bara. Single phase fluid at 60°C was displaced through the core at rates in excess of 10 L/h at an inlet pressure of 231 bara. The measured data are presented in Figure 9. (The extrapolated low rate flood data corresponds to the measured reference permeability of 67.7 md). Non-Darcy flow was apparent at rates of 3 L/h but became significant at rates in excess of 6 L/h. The measured pressure data as a function of rate were analysed using equation 7 of Evans et al [5]. Figure 10 shows the results which give a gas permeability of 69 md and a β coefficient of 4.8×10^8 m^{-1}.

6.2 Test 2 : Reservoir Fluid at ~170 bara

For the second test, the core and the outlet 15 L accumulator were depressurised to a 'bottom hole pressure' (BHP) of ~160 bara. At this pressure the fluid was at maximum liquid saturation with an IFT of approximately 0.8 mN/m. The 'reservoir fluid' contained in the inlet 15L accumulator was depressurised to ~170 bara, so that the composition of the gas was lean, but not fully depleted. The reservoir fluid was displaced through the core following a ~ 10 barg flash across the inlet pressure reducing regulator. The displacement was continued until a steady-state differential pressure, condensate production and total production rates were observed. Once steady-state values were measured, a new displacement rate was established by lowering the BHP by ~1 barg (using the outlet back-pressure regulator). New steady-state conditions were established rapidly, typically in much less than 0.5 hour. For the first near well test, it was possible to undertake four displacement rates before the reservoir fluid expired (~8 Litres of lean fluid at 170 bara). The results of measured pressure drop versus flowrate are presented as 'hr_170' in Figure 11.

6.3 Tests 3 & 4 : Reservoir Fluid at ~190 & ~224 bara

Prior to test 3 (and later test 4) it was necessary to re-establish single phase conditions. This involved revaporising all liquid components throughout the system and mixing the liquid with its associated gas. With the fluid revaporised, the core low rate reference permeability and fluid CVD characteristics were measured as a means of quality checking. The third test was undertaken by again depleting the core to a BHP of ~160 bara. The reservoir fluid was depressurised to ~190 bara, thus making the reservoir fluid composition richer than test 2. The test procedure was repeated, establishing steady-state conditions at 10 displacement rates (using ~11 Litres of gas at ~190 bara). Results from this experiment are shown as 'hr_190' in Figure 11. To obtain some idea of data reproducibility using the high rate flow circuit, two displacements were undertaken at 0.335 L/h, 3 days apart, and identical steady-state data were obtained. A lower rate flood was also undertaken following a period of higher rate flooding (rates up to 2.358 L/h). The measurements obtained were consistent, indicating that there was no hysteresis effect resulting from the rate changes.

For the fourth and last test, the core was again depleted to a BHP of ~160 bara, but the reservoir fluid was kept single phase at an inlet accumulator pressure of ~224 bara. Using this fluid required a 64 barg flash across the inlet pressure reducing regulator to the inlet pressure of 160 bara. Once again, no hysteresis was observed in the data for the 'low rate' measurements undertaken after flooding at the highest rate (4.3 L/h). Results from this experiment are shown as 'hr_224' in Figure 11.

6.4 Measurement of Reference Permeability

The measurements of low rate reference permeability (using unadulterated, single phase 5-component fluid) were undertaken between each test. The initial reference permeability was 67.7 md (at a measured S_{wi} of 0.118 PV). After the first test to measure β using the single phase fluid (and before depressurisation of the core) the reference permeability was measured as 75.1 md. This permeability was remeasured after the

second test (hr_170) as 82.1 md and again after the third test (hr_190) as 86.8 md. On completion of the final test, the core was restored to refined oil (heptane) at a measured S_{wi} of 0.031 PV and the effective oil permeability was measured as 99.5 md. These reference permeability measurements are an indication that water is removed from the core. This observation may be expected for tests 2 to 4, since the reservoir fluid will be in equilibrium with water at the inlet accumulator pressure, and when the fluid flashes to core conditions, it has the capacity to vaporise additional water to reach equilibrium at the lower pressure. The effect should be less pronounced in test 1, since the relatively small core differential pressure and gas throughput only has a small capacity to vaporise additional water.

6.5 Using Relative Permeability Data to Calculate Well Deliverability

Gas condensate well productivity can be calculated using a compositional reservoir simulator with small grid cells around the well. Many compositional simulators now include options for modelling capillary number effects, based on empirical correlations for relative permeability as a function of gas saturation and capillary number. Reference [6] includes a review of the different correlations which have been proposed.

The experimental technique described in this paper produces data for k_{rg} as a function of k_{rg} / k_{ro} and capillary number. We have used a spreadsheet to calculate data in this form, starting from correlations in terms of gas saturation. The parameters in the correlation were then adjusted to optimise the fit to the measured data. This procedure is discussed in more detail in reference [7]. An alternative way to use the data from this type of experiment is in a pseudopressure calculation [1] either within a reservoir simulator, or in a material balance calculation [8]. The pseudopressure calculation only needs to calculate k_{rg} as a function of k_{rg} / k_{ro} and capillary number, so that the experimental data can be used directly.

7. DISCUSSION

The objective of the x-ray in-situ saturation monitoring was to quantitatively measure saturations in various condensate systems. The preparation work completed in the condensate drainage test and other tests has allowed us to refine the techniques so that these experiments can be performed without dopants. The techniques developed will enable measurement of condensate saturation distributions during the steady-state near well bore experiments which are currently ongoing. The in-situ data from the drainage tests showed that condensate drainage can occur over distances of 1 m in only 10 days, demonstrating the scope for significant drainage within the timescale of field developments. Relative permeabilities were estimated from the saturation profiles and it is interesting to note that they were two orders of magnitude higher at low condensate saturation than those deduced from gravity drainage experiments using analogue fluids [9].

The condensate drainage study graphically demonstrates the advantage of using in-situ saturation measurements to aid interpretation of the processes occurring within the core. Volumetric measurements in the PVT cell would suggest that no condensate drainage occurred, whereas the in-situ data has clearly shown that drainage did occur, forming a condensate bank at the core outlet. Information of this kind will be valuable for the correct interpretation of data derived from the near well bore experiments. Early measurements indicate that the x-ray scanner accuracy will be sufficient to gain quantitative saturation data.

The near well bore flow circuit has in practice provided a very effective means of measuring gas condensate relative permeability. The simplicity of the technique enables steady-state data to be acquired very quickly, and there are significant advantages over conventional steady-state measurements. Some key points are:

(a) Steady-state is achieved quickly, typically much less than 0.5 hour, and it is straight forward to measure core differential pressure, steady-state liquid production and total displacement rate; the 3 parameters required for the calculation of k_{rg} and k_{ro}.

(b) Selection of reservoir fluid pressure i.e. fluid composition and ‘BHP’ (core pressure) enable flowing conditions to be flexible and tailored to specific, near-well situations generating relative permeability data with the right fluid viscosity and IFT.

(c) The current technique is only practicable for differential pressures exceeding ~5 psi. This is due to the resolution on the pressure regulators being 0.1 bar, and sufficient core differential pressure is required to discriminate from the operational noise exhibited by the controllers. To obtain k_{rg} and k_{ro} data at low capillary number, conventional steady-state techniques will be required or high rate operations at much higher IFT.

(d) The technique is a single pass operation; fluid recycling is not possible as the composition of the reservoir fluid changes from the inlet conditions to the core conditions. Large fluid volumes are therefore required. To obtain a data series of 5 to 10 steady-state points would require a reservoir fluid volume of approximately 5 to 10 L.

(e) Although acquisition of data is very quick, fluid handling may prove to be expensive and/or time consuming for real reservoir fluid systems. These limitations may be reduced in time with more experience and specialised equipment tailored to the technique.

The effects of non-Darcy flow are very real and apparent in Figure 9, with core differential pressure rising disproportionately with increasing displacement rate (permeability is decreasing with rate). However, the magnitude of the non-Darcy effect is less than that of capillary number. This is evident in Figure 11, where the differential pressure decreases disproportionately with increasing displacement rate (permeability is increasing with rate). The near well bore relative permeability data has been plotted as a function of capillary number in Figure 12, where capillary number is defined as the superficial gas velocity multiplied by gas viscosity divided by IFT. Viscosity and IFT at test conditions were predicted from PVT simulation and adjusted to match measured values at 40°C. The fitting of correlations to these experimental data is presented in detail in reference [7].

ACKNOWLEDGEMENTS

The authors wish to express their gratitude and acknowledge our Sponsors for their permission to allow us to present this work : Amoco (UK) Exploration Company, BP Exploration (now BP-Amoco), U.K. Department of Trade & Industry, Esso UK E&P, Marathon Oil UK Ltd, Mobil North Sea, Phillips Petroleum Company UK Ltd, SAGA Petroleum, Texaco Britain Limited.

REFERENCES

1. Fevang, O., Whitson,C. ‘Modelling Gas Condensate Well Deliverability’, SPE Res Eng, November 1996, p221-230.
2. Afidick, D, Kaczorowski, N.J, and Bette, S.. ‘Production Performance of a Retrograde Gas Reservoir: A Case Study of the Arun Field’. SPE 28749, SPE Asia Pacific Oil and Gas Conference, November 1994.
3. Diamond, P.H. et al. ‘Probabilistic Prediction of Well Performance in a Gas Condensate Reservoir’. SPE 36894, presented at the SPE European Petroleum Conference, Milan, 22-24 October 1996.
4. Naylor, P., Puckett, D. A. ‘In-Situ Saturation Distributions: The Key to Understanding Core Analysis’, SCA-9405, presented at Society of Core Analysts Symposium, Stavanger, September 1994.
5. Evans, R.D. *et al*, ‘The Effect of an Immobile Liquid Saturation on the Non-Darcy Flow Coefficient in Porous Media’, SPE Prod Eng, p 331-338 November.
6. Blom, S.M.P. and Hagoort, J. ‘How to Include the Capillary Number in Gas Condensate Relative Permeability Functions?’ SPE 49268, SPE Annual Technical Conference and Exhibition, October 1998.
7. Mott, R., Cable, A. and Spearing, M. ‘A New Method for Measuring Relative Permeabilities for Calculating Gas Condensate Well Deliverability’, SPE 56484, to be presented at the SPE Annual Technical Conference and Exhibition, Houston, 3-6 October 1999.
8. Mott, R. 'Calculating Well Deliverability in Gas Condensate Reservoirs', to be presented at the 10th European Symposium on Improved Oil Recovery, Brighton, UK, 18-20 August, 1999.
9. Fishlock, T., Jones, P., Mead, B., Spearing, M., and Todd, J. ‘Implications of Condensate Drainage for Field Development Strategies: A Laboratory and Simulation Study’, presented at IEA Collaborative Project On EOR, 18th Int. Workshop and Symposium, Copenhagen, Denmark, September 1997.

FIGURE 1: Gas Condensate Module / x-ray Scanner

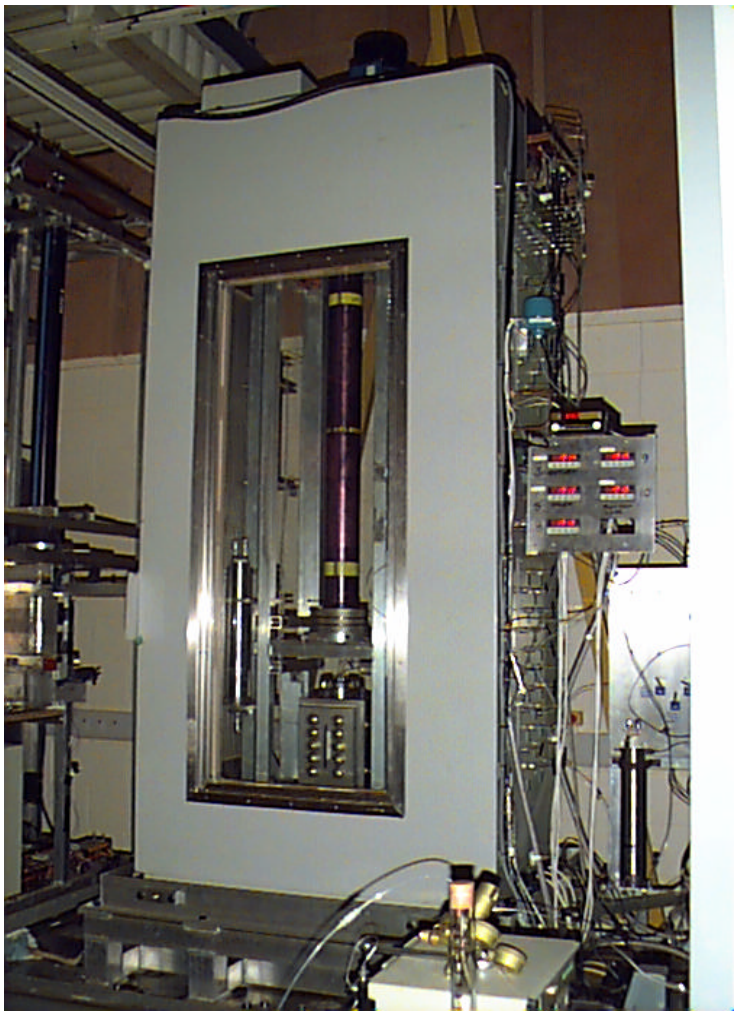

FIGURE 2: Schematic Diagram Condensate Module Flow Circuit

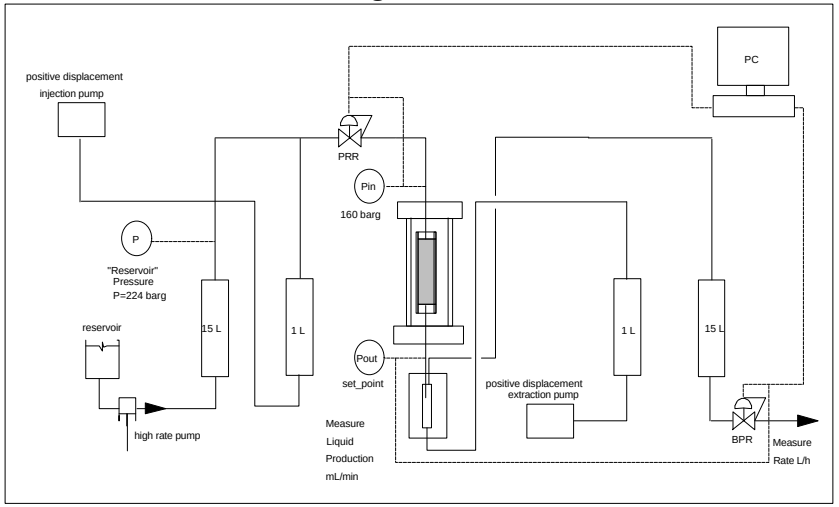

FIGURE 3: Schematic Diagram of the X-ray Scanner

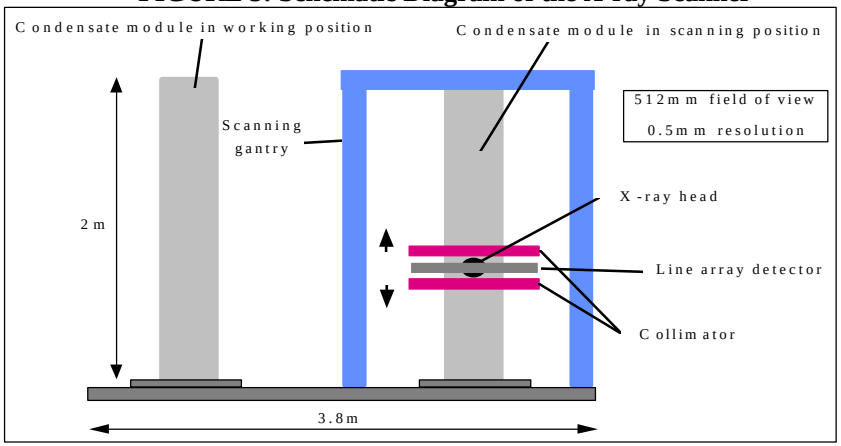

FIGURE 4: 3-phase x-ray saturation accuracy. 5-component synthetic condensate and 3%NaI doped brine at 60 degC

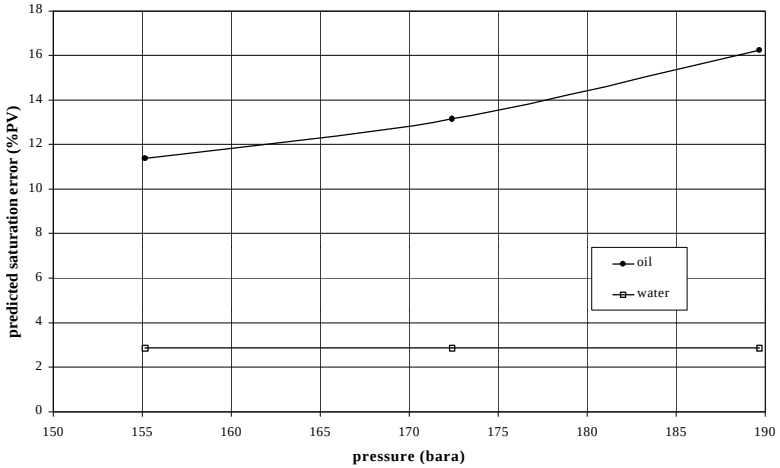

FIGURE 5: 2-phase x-ray saturation accuracy. Undoped 5-component synthetic condensate at 60 degC

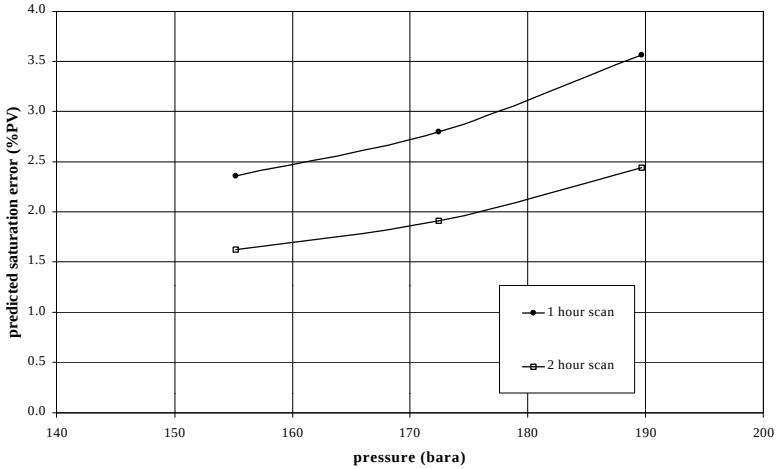

FIGURE 6: Predicted CCE and measured CVD

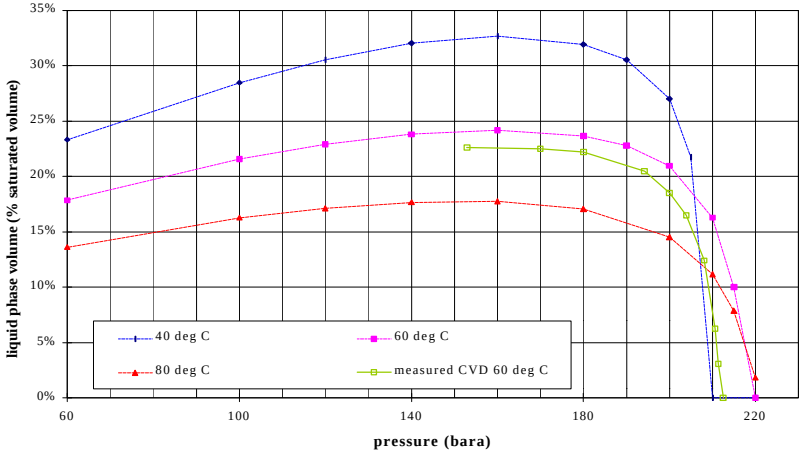

FIGURE 7: Measured condensate saturation

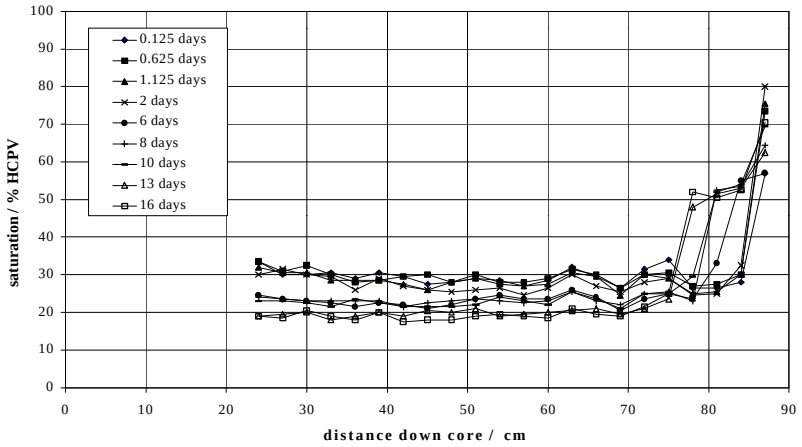

FIGURE 8: X-ray images showing condensate drainage

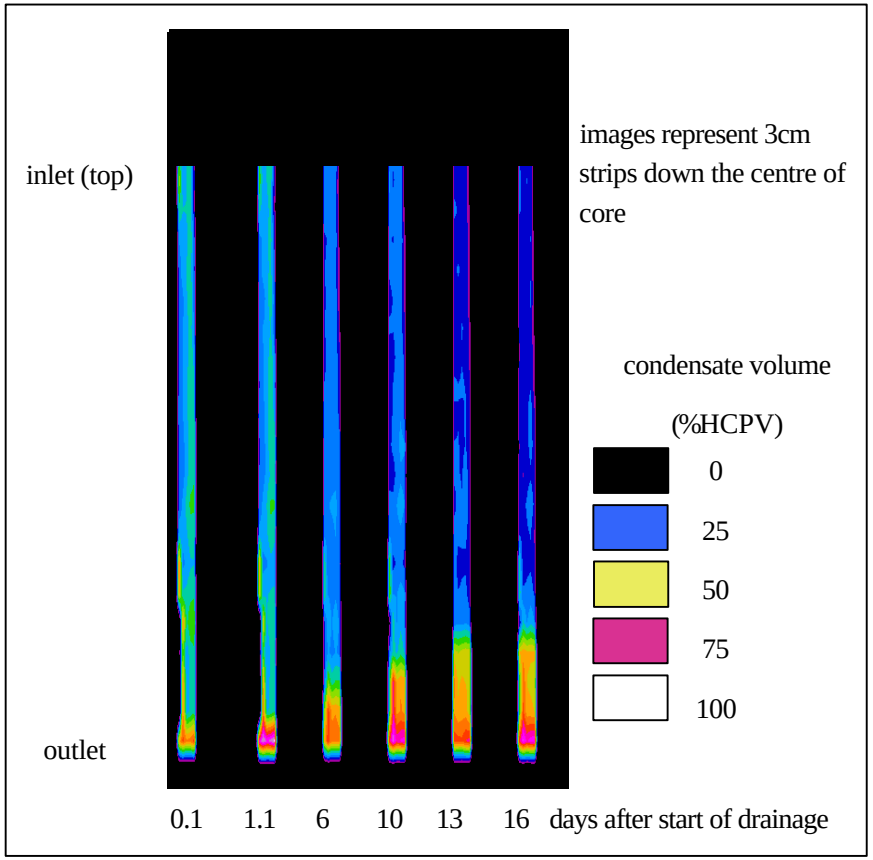

FIGURE 9: Pressure versus flowrate (test 1)

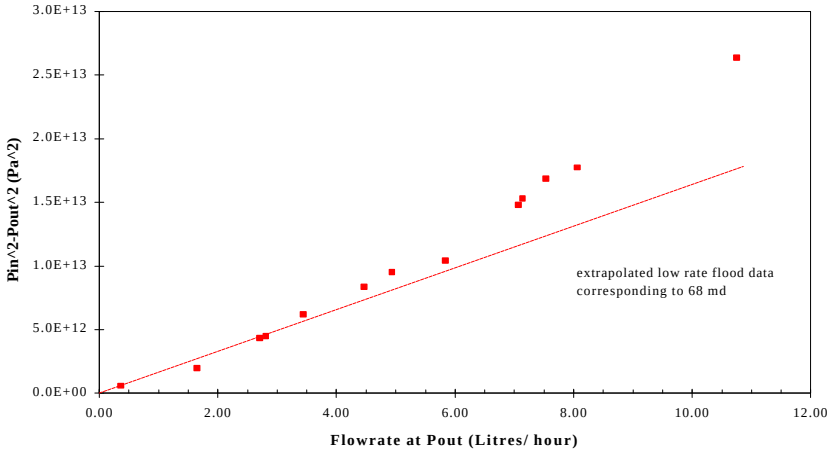

FIGURE 10: Permeability using analysis of Evans et al

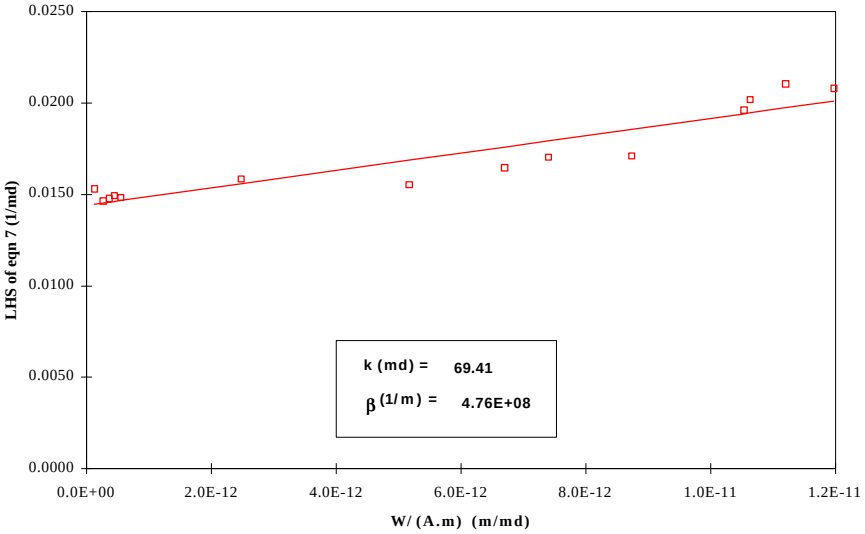

FIGURE 11: Pressure versus flowrate (tests 2-4)

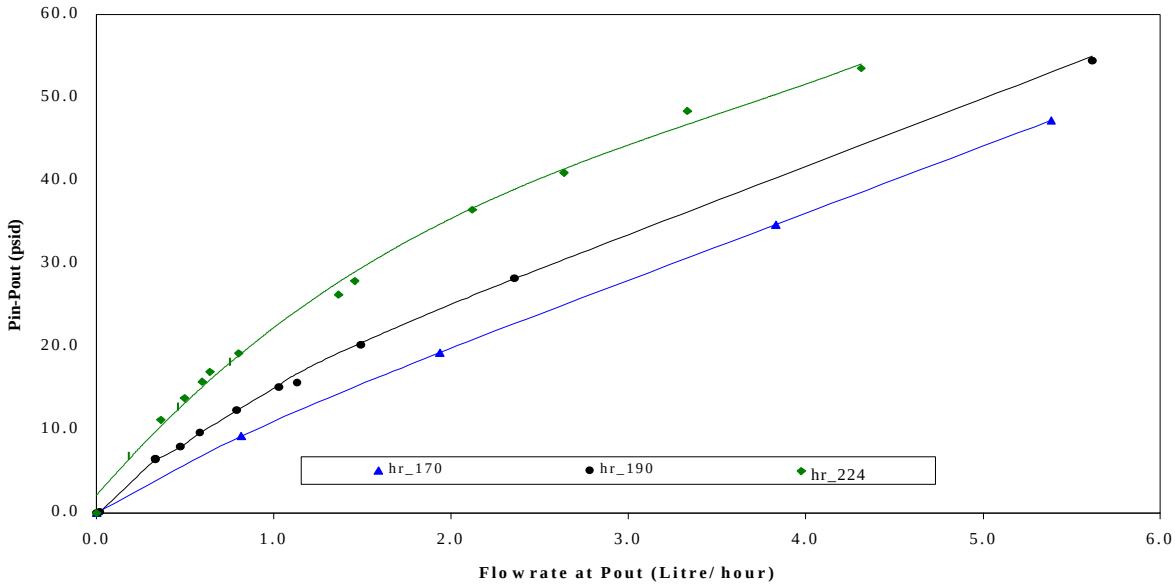

FIGURE 12: Relative permeability versus capillary number